Synthetic Metals 307 (2024) 117678

Contents lists available at ScienceDirect

Synthetic Metals

journal homepage: www.elsevier.com/locate/synmet

Diketopyrrolopyrrole based molecular semiconductors with intrinsic conductivity

Lewis M. Cowen [a,*], Megan M. Westwood [a], Pauline M.F. Kasongo-Ntumba [b], Irena Nevjestic [c], Peter A. Gilhooly-Finn [a], Sandrine Heutz [c], Oliver Fenwick [b], Bob C. Schroeder [a,*]

[a] Department of Chemistry, University College London, 20 Gordon Street, London WC1H 0AJ, UK
[b] School of Engineering and Materials Science, Queen Mary University of London, London E1 4NS, UK
[c] Department of Materials and London Centre for Nanotechnology, Imperial College London, SW7 2AZ, UK

ARTICLE INFO

Keywords:
Molecular conductors
Self-doping
N-type
Structural analysis
Hydrolysis

ABSTRACT

Intrinsically conducting diketopyrrolopyrrole (DPP) compounds functionalised with pendant quaternary ammonium groups have been synthesised. The hydroxide forms were found to be the product of base hydrolysis of the DPP amide during synthesis, likely made possible by restricted resonance. This gave mixed chemical compositions of solutions and conductive films formed by drop-casting. Chemical decomposition of the hydrolysed compounds was also observed at temperatures above 85 °C. Conductivities of approximately 3×10^{-4} S m^{-1} were observed in processed films of DPP ammonium hydroxides. It was also found that trifluoroacetic acid (TFA) DPP precursors gave clear electron paramagnetic resonance (EPR) signals indicative of doping and exhibited conductivities one order of magnitude larger than the hydroxides. This opens the possibility of using ammonium TFAs as moieties for doping organic semiconductors.

1. Introduction

Since the observation of increased conductivity in films of polyacetylene when exposed to halogen vapours [1] doping of organic semiconductors has increased the potential for their application in multiple technologies. Advancements in the doping of organic light emitting diode (OLED) active materials has increased device efficiencies to the point of industrialisation [2–4]. Doping has been employed to improve the efficiency of organic field effect transistors (OFETs), this can be through modulation of the Fermi-level in order to improve Ohmic contact [5] or increase charge mobility [6–8], or through filling of trap-states [7]. Advancements in organic photovoltaics (OPVs) have been achieved when doping the bulk heterojunction (BHJ) [9,10] or interlayers [11] and the field of organic thermoelectrics is reliant on the generation of free charge carriers through doping [12–14].

In the decades since polyacetylene was doped with halogens both material design and processing techniques have become more sophisticated. The introduction of molecular dopants means that the full scope of organic synthesis can be employed to generate high performing dopant-semiconductor pairs through tuning of energy levels and intramolecular interactions [15]. With well considered processing of films for microstructure [16,17], highly optimised doped organic systems can now be generated. Efficient p-type materials include PEDOT-PSS [18,19], polythiophene derivatives [20,21], polypyrroles [22,23] and more [24–26]. The practical application of organics has been slowed however by the relative difficulties in developing ambient stable n-doped systems. Promising n-type systems have mostly been limited to naphthalenetetracarboxylic diimide (NDI) [27–30] and benzodifurandione-phenylenevinylene (BDPPV) [31,32] polymers doped with 4-(1,3-dimethyl-2,3-dihydro-1-*H*-benzoimidazol-2-yl) phenyl)dimethyl-amine (N-DMBI) [33–35] and its derivatives.

Introducing extrinsic molecular dopants however requires optimisation of the processing techniques to avoid disruption of the semiconductors structural order [16,17]. In addition to this, dopants can coulombically trap charge carriers [36]. Intrinsic doping has proved to be an effective strategy in the development of stable n-type organic conductors. This involves covalently binding a doping moiety to an electron deficient conjugated core. Common doping moieties used are quaternary ammonium hydroxides, with rylene diimides used as the conjugated core, a generalised structure is shown in Fig. 1 [37–42].

Self-doping rylene diimides show promise due to their remarkable ambient stability when doped, as well as water solubility allowing for

* Corresponding authors.
E-mail addresses: lewis.cowen.17@ucl.ac.uk (L.M. Cowen), b.c.schroeder@ucl.ac.uk (B.C. Schroeder).

https://doi.org/10.1016/j.synthmet.2024.117678
Received 7 December 2023; Received in revised form 1 May 2024; Accepted 8 June 2024
Available online 9 June 2024

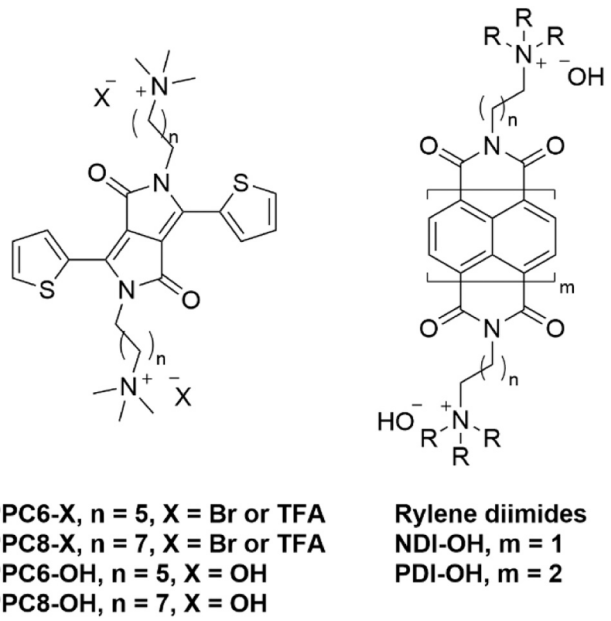

Fig. 1. Structures of self-doping diketopyrrolopyrroles **DPPC6-OH** and **DPPC8-OH**, and their precursors **DPPC6-X** and **DPPC8-X**. Also shown is a general structure for previously studied self-doping rylene diimides NDI-OH and PDI-OH.

processing from an aqueous solution. The exact mechanism of doping is still under investigation with multiple possibilities for quaternary ammonium hydroxide group degradation such as Hofmann [43–45] or demethylation [41]. It has recently been suggested however that ammonium degradation is immaterial with respect to the doping mechanism following the observation of water inhibiting the n-doping of multiple perylenediimide tetracarboxylates (PDIs) [42]. This supports the suggestion that n-doping is driven by deshielding of anions after dehydration, leading to an electron transfer on to the more polarisable aromatic ring [39].

We have previously shown that exposure to highly basic conditions during synthesis lead to ring-opening hydrolysis of the imide group which further complicates the study of the doping mechanism [46]. Another conjugated core, not containing imide groups, which has exhibited intrinsic n-doping behaviour is diketopyrrolopyrroles (DPP). Electron paramagnetic resonance (EPR) signals have been reported for DPP covalently bound to a dimethylamine group [41] and ammonium salts of DPPs have exhibited self-doping while used as solar cell interlayers [47]. Intrinsic doping in ammonium hydroxide salts of DPP however have not been studied.

In this study we have designed and synthesised diketopyrrolopyrrole (DPP) molecular semiconductors functionalised with quaternary ammonium hydroxide sidechains. The structures of **DPPC6-OH** and **DPPC8-OH**, as well as their precursors **DPPC6-X** and **DPPC8-X**, are shown in Fig. 1. The amide group in DPPs is, intuitively at least, less prone to hydrolysis than the imides of rylene diimide. These compounds could therefore provide an insight into the mechanism of doping in ammonium hydroxide salts without the added complication of ring-opening hydrolysis reactions. In addition, DPP molecular and polymeric derivatives have previously exhibited promising n-type properties when doped extrinsically [48,49]. It is necessary to optimise the interactions between dopant and semiconductor in these systems however, and an intrinsically doping DPP could drastically reduce the processing costs involved in producing organic and hybrid devices.

2. Results

2.1. Synthesis and structural characterisation

The synthetic routes toward the two compounds **DPPC6-OH** and **DPPC8-OH** are shown in Scheme 1. Thienyl-DPP (**3**) was chosen as the aromatic component due to its ease of synthesis and ubiquitous nature across organic electronics research [50–52]. Additionally, thienyl-DPP units were previously suggested to undergo intramolecular electron transfer when functionalised with tertiary amine groups [41] or ionic ammonium bromides and ammonium borates [47]. **3** was synthesised via ring-closing condensation using diethyl succinate and thiophene-2-nitrile. Base catalysed alkylation with 1,6-dibromohexane or 1,8-dibromooctane gave the compounds **4** and **5**.

Quaternary ammonium salts were obtained by reaction of **4** and **5** with the salt trimethylamine hydrochloride [53] to give the compounds **DPPC6-Br** and **DPPC8-Br**. Purification was carried out by preparative high-pressure liquid chromatography (HPLC) with solvents spiked with 0.1 % trifluoroacetic acid. After lyophilisation, ^{13}C NMR analysis (Figures S3 and S6) showed two unexpected shifts for both compounds at 163 ppm (quartet) and 117 ppm (quartet). These match closely to the carbons of trifluoroacetate (TFA) ions [54]. It was assumed that these shifts are not from residual trifluoroacetic acid due to their presence after lyophilisation, with protonated TFA commonly being removed from peptides by lyophilisation [55]. The bromide counterion of **DPPC6-Br** and **DPPC8-Br** was exchanged for TFA, at least partially, during HPLC purification. Since the aim was to study the hydroxide forms after exchange of counterion, it was determined that the precursor containing a possible mixture of TFA and bromide could be carried forward and named **DPPC6-X** and **DPPC8-X**.

In keeping with previous attempts at forming the ammonium hydroxide moiety, for intrinsic dopants, the precursors **DPPC6-X** and **DPPC8-X** were eluted through a column of hydroxy-form ion-exchange resin. Performing this ion-exchange column in D_2O allows for the eluent solution to be analysed by nuclear magnetic resonance (NMR). When this same analysis was performed on an NDI derivative (**NDI-OH**) it was found that the imide group had undergone a base catalysed ring-opening hydrolysis during the ion-exchange procedure [46]. After heating, both in solution or during dehydration in film formation, the hydrolysis was partially reversible leading to mixed chemical compositions of films formed at different temperatures. Fig. 2 shows the aromatic region of solution ^{1}H NMR spectra of **DPPC6-OH** and **DPPC8-OH** after elution of **DPPC6-X** and **DPPC8-X** through ion-exchange resin in D_2O. Full spectra as well as ^{13}C and 2-dimensional correlation spectra are shown in Figures S8 to S21.

Fig. 2 shows two doublets and a doublet of doublets (approx. 8.4, 7.8 and 7.2 ppm) corresponding to the three thiophene protons of **DPPC6-X** and **DPPC8-X**. Similar signals are observed in the hydroxide derivatives **DPPC6-OH** and **DPPC8-OH** as well as at least five further signals in the aromatic region. The additional signals present in the two hydroxide derivatives can be reasonably assigned to a ring-opened mono-hydrolysed product **6** (Scheme 3). The doublets at approximately 7.91 ppm and 7.57 ppm may correspond to the thiophenes of a relatively minor amount of di-hydrolysed product. ^{1}H–^{1}H correlations (COSY) for the ring-closed and ring-opened DPP structures are highlighted in Figures S13, S14, S20 and S21.

To the extent of our knowledge this ring-opening has not been observed in DPP compounds and may be due to restricted resonance of the DPP ring (Scheme 2). The energy normally associated with this resonance is 15–20 kcal mol^{-1} and is responsible for the stability of planar amides [56,57]. Exceptions to this stability include *N*-acylimidazoles [58–60] and *N*-acylpyrroles [61,62] in which reactions such as base catalysed hydrolysis are observed. This is due to the restricted resonance preserving aromaticity and subsequently increasing the electrophilicity of the carbonyl carbon. DPP does not necessarily meet all criteria to be considered aromatic [63], however and the dominance

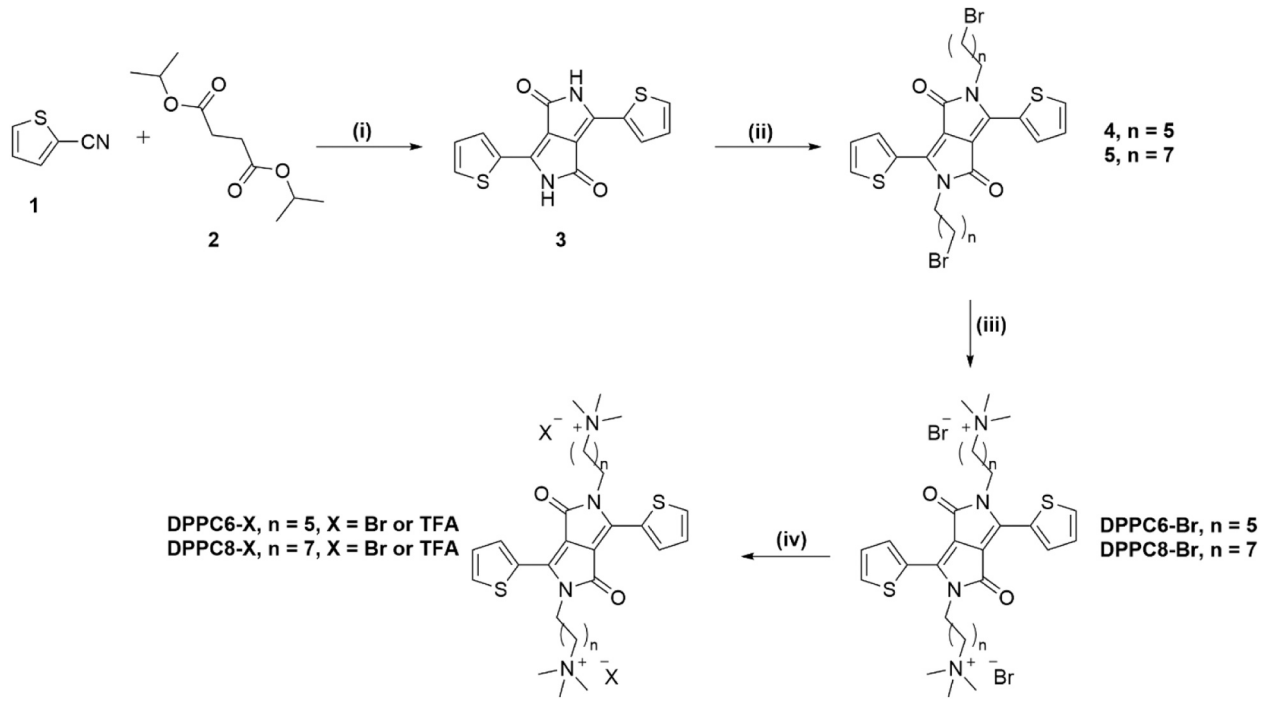

Scheme 1. Synthesis of **DPPC6-X** and **DPPC8-X**. Reagents and conditions: (i) *t*-BuOK, *t*-amyl alcohol, reflux 4 h, 58 % (ii) Cs_2CO_3, MeCN, reflux 12 h, **4** dibromohexane 23 %, **5** dibromooctane 10 % (iii) NMe_3.HCl, $NaHCO_3$, MeCN, 80 °C, 24 h (iv) HPLC in H_2O, MeCN and TFA, **DPPC6-X** 13 %, **DPPC8-X** 17 %.

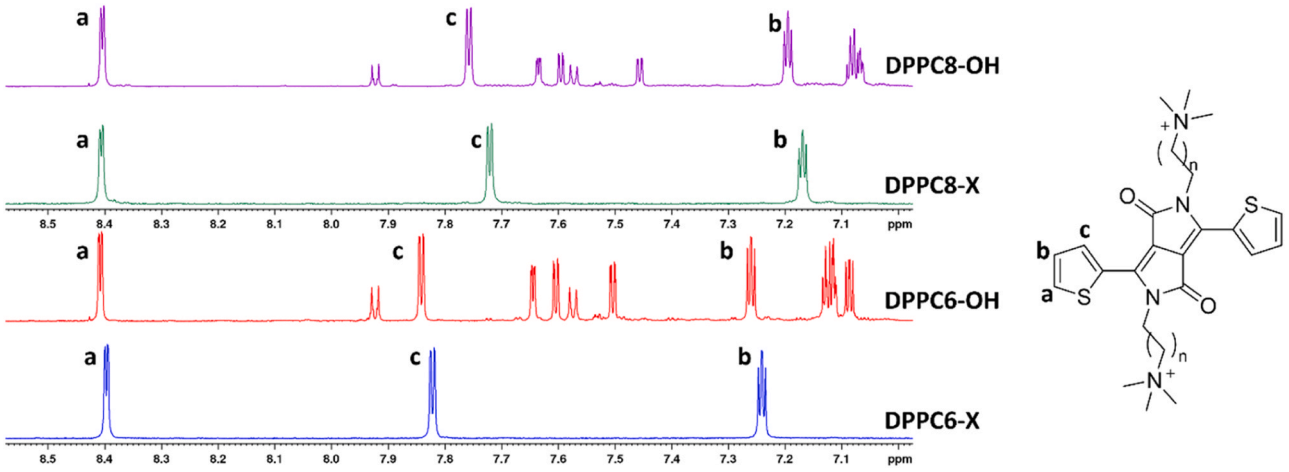

Fig. 2. Overlays of solution ^{1}H NMR spectra of **DPPC6-X**, **DPPC6-OH**, **DPPC8-X** and **DPPC8-OH** in deuterium oxide in the region between 7.0 ppm and 8.5 ppm. Thiophene protons of the ring-closed structure are highlighted in all four spectra.

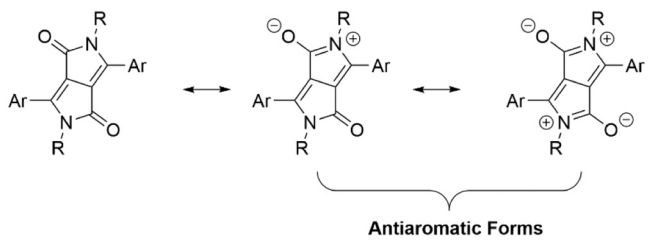

Scheme 2. Amide resonance forms applied to DPP.

of the lactam form (left structure, Scheme 2) may come from an increased planarity in the lactim (middle and right structures, Scheme 2) causing unfavourable antiaromaticity in the ground state. This is supported by calculations which have shown that excited state DPP adheres to Baird's rule of aromaticity (4 n π-electrons) [64].

The relative inertness of amide groups compared to imides, when considering hydrolysis, lead us to believe that DPP cores may offer a route to observing the self-doping mechanism without the complication of reversible hydrolysis reactions. As shown in Fig. 2 however it is clear a chemical mixture was present in **DPPC6-X** and **DPPC8-X**. To identify if the chemical mixture present in solution had any effect on the composition of thin films, **DPPC6-OH** and **DPPC8-OH** were drop-cast at temperatures of 45 °C, 85 °C and 125 °C and redissolved in D_2O for ^{1}H NMR analysis. A comparison of the aromatic regions of spectra for **DPPC6-X**, **DPPC6-OH** and the three redissolved films of **DPPC6-X** are shown in Fig. 3. The full spectra of redissolved films are shown in Figures S22 to S27 along with spectra for **DPPC8-OH**.

Redissolved films drop-casted at 45 °C gave similar NMR spectra to the solution of **DPPC6-OH**. The integrated peak areas for the ring-closed DPP (δ; 7.28, 7.85 and 8.43 ppm) increased, relative to the mono-

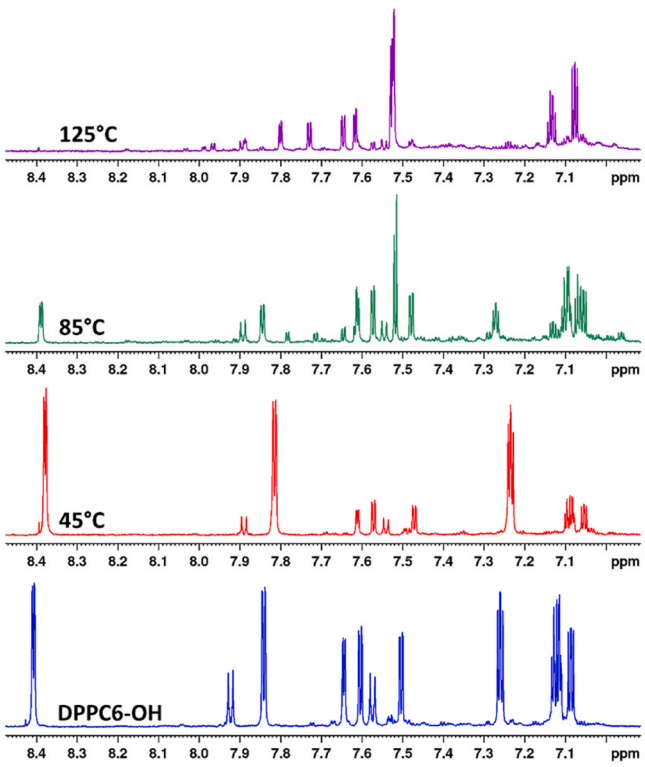

Fig. 3. Overlays of solution ^{1}H NMR spectra of **DPPC6-OH** in deuterium oxide with solution ^{1}H spectra for redissolved thin-films of DPPC6-OH drop-cast at 45°C, 85°C and 125°C in deuterium oxide.

hydrolysed compound **6**, in the 45 °C film when compared to the **DPPC6-OH** solution. This is indicative of a thermally activated reversal of hydrolysis (Scheme 3) which was also observed in films of NDI [46]. On increasing the drop-casting temperature to 85 °C the relative intensities for the mono-hydrolysed compound **6** increased compared to the ring-closed signals. Multiple additional peaks of unknown origin were also observed. At 125 °C, the signals for **DPPC6-OH** almost completely disappeared and were replaced by unassignable peaks initially observed at drop-cast temperatures of 85 °C, thus exemplifying the dynamic nature of the chemistry occurring during film formation at elevated temperatures.

A summary of the chemical changes undergone by **DPPC6-OH** and **DPPC8-OH** is given in Scheme 3. The changing nature of the NMR spectra in Fig. 3 shows that ring opened DPP compounds were subject to a reversal of hydrolysis under mild heating (45 °C) and dehydration. Increasing the temperature of drop-casting (>85 °C) began a decomposition process in both **DPPC6-OH** and **DPPC8-OH**. It is difficult to clarify if this onset of breakdown was accompanied by further hydrolysis and ring-opening. Drop-casting at temperatures of 125 °C led to almost complete breakdown and no presence of the DPP could be detected at these drop-casting temperatures.

Relative amounts of the various compounds formed within the films can be estimated by integrating the corresponding peak areas in the ^{1}H NMR spectra. An attempt at quantifying the extent of the hydrolysis reaction after ion-exchange (**DPPC6-X**/**DPPC8-X** → **6**) and subsequent reversal after drop-casting at 45 ºC (**6** → **DPPC6-OH**/**DPPC8-OH**) using relevant NMR peak integrations is outlined in Table 1 in the supporting information. A significant amount of **6** was formed on exposure to the ion-exchange resin, 55 % for **DPPC6-X** and 40 % for **DPPC8-X**. At drop-casting temperatures of 45 ºC, the hydrolysis is largely reversed with only 26 % of **6** remaining for **DPPC6-OH** and 12 % of **6** for **DPPC8-OH**. It was then necessary to examine the effect this shifting chemical composition had on any doping of the DPP cores.

2.2. *Intramolecular doping*

Intramolecular n-type charge transfer has recently been observed in a DPP compound conjugated with triphenylamine (TPA) groups [65], as well as in DPPs bound to ammonium bromides and ammonium borates [47]. Fig. 4 shows a summary of UV–visible (UV–vis) absorption spectra, used here for initial observations in charge transfer after ion-exchange in solution or in dehydration of solutions when drop-casting films at various temperatures. Solution spectra for **DPPC6-X** and **DPPC8-X** (Fig. 4, left) exhibit two absorption maxima at 350 nm and 510 nm, consistent with absorption spectra for molecular thienyl-DPPs [66]. Absorption spectra for **DPPC6-OH** and **DPPC8-OH** (Fig. 4, left) exhibit the same peak maxima however a small absorption can also be observed between approximately 370 and 420 nm. This may be due to aggregation effects in polar solvents as similar features have previously been observed in absorption spectra run in methanol solutions [65]. It is possible however that the monohydrolysed structure **6** has differing optoelectronic properties. Time-dependent density functional theory (TD-DFT) calculations in Figure S28 indicate that the ring-opened DPP **6** gives rise to a blue shifted absorption (approx. 400 nm), which may explain the peak between 370 and 420 nm in **DPPC6-OH** and **DPPC8-OH** solution spectra.

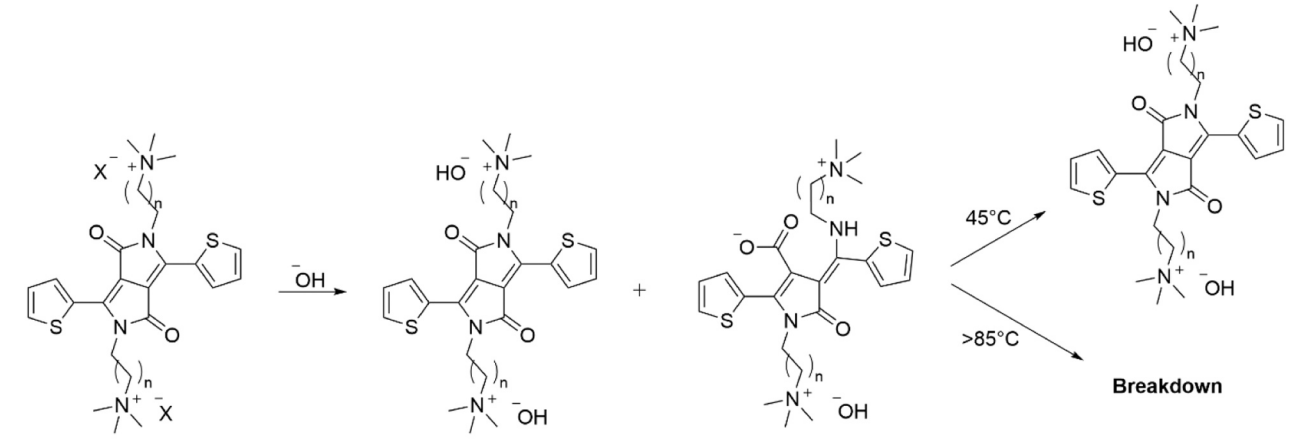

Scheme 3. Hydrolysis under ion-exchange conditions followed by reversal.

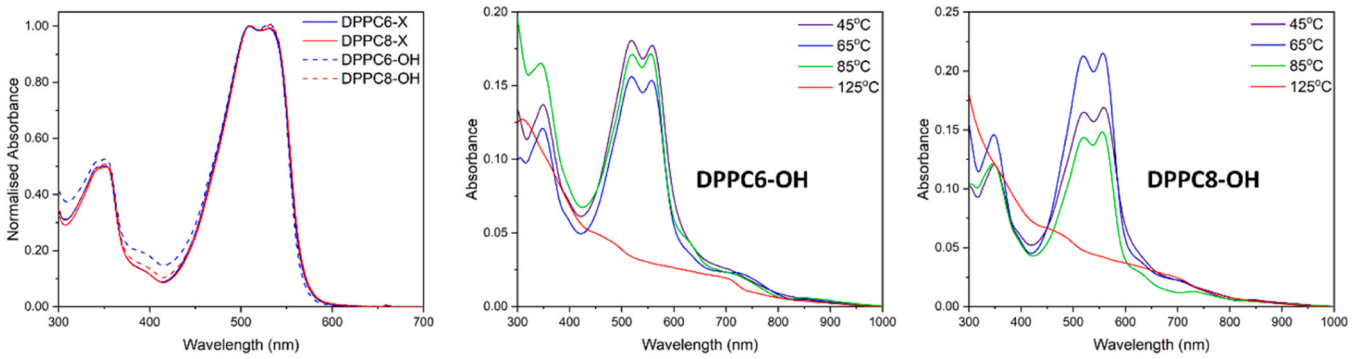

Fig. 4. Solution UV–vis absorption spectra of **DPPC6-X**, **DPPC8-X**, **DPPC6-OH** and **DPPC8-OH** in water (left). Thin-film UV–vis absorption spectra of **DPPC6-OH** (middle) and **DPPC8-OH** (right) drop-cast at temperatures of 45°C, 65°C, 85°C and 125°C.

Self-doping of rylene diimides by quaternary ammonium hydroxide groups has previously been triggered by dehydration of the aqueous solution by drop-casting to form thin-films and subsequently annealing [39–42,46]. Solutions of **DPPC6-OH** and **DPPC8-OH** were drop-cast at temperatures of 45, 65, 85 and 125 °C. Middle and right panels of Fig. 4 show that the absorption features of films drop-cast between temperatures of 45 and 85 °C were mostly dominated by the ring-closed DPP structures (maxima at 350 and 510 nm). A small tail in the absorption for films at these temperatures was also observed between 700 and 800 nm, which may be the first indication of lower energy polaron like states caused by intramolecular charge transfer [67]. Films drop-cast at 125 °C showed no definitive absorption features and is further evidence of breakdown in the DPP ring structure at high temperatures.

To aid in confirming if electron transfer has taken place on to DPP, electron paramagnetic resonance (EPR) spectroscopy of drop-cast films has been utilised and results are shown in Fig. 5. Films drop-cast at 125 °C are not included due to the observation of breakdown of the DPP structure at these temperatures.

All samples were drop-cast and measured in air. Samples of **DPPC6-X** at 45 °C show a wide broad signal centred at around 315 mT. The broad nature of this signal makes it difficult to fully assign. When drop-cast at 65 °C this signal is no longer present in **DPPC6-X** but a sharper signal is resolved at around 315 mT in films at 85 °C. Films of **DPPC8-X** exhibit a signal around 332 mT for drop-casting at 45 °C which decreases in intensity significantly at 65 °C and 85 °C. A low intensity broad signal around 315 mT is also present at these higher temperatures. Both

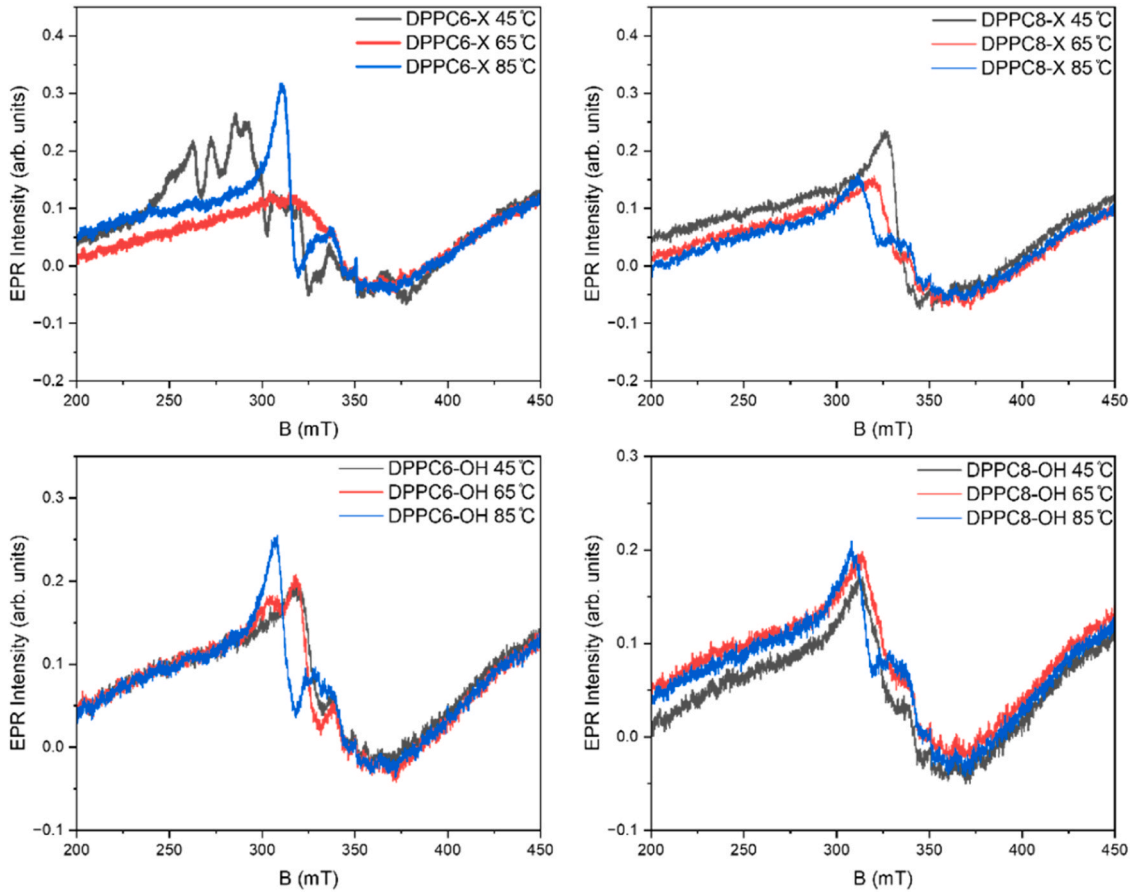

Fig. 5. EPR spectra of **DPPC6-X** drop-cast at temperatures of 45, 65 and 85 °C (top-left), **DPPC8-X** drop-cast at temperatures of 45, 65 and 85 °C (top-right), **DPPC6-OH** drop-cast at temperatures of 45, 65 and 85 °C (bottom-left) **DPPC8-OH** drop-cast at temperatures of 45, 65 and 85 °C (bottom-right).

DPPC6-OH and **DPPC8-OH** exhibit a signal around 332 mT whereas films formed by drop-casting at 85 °C present a sharper signal at around 315 mT, similar to the TFA precursors.

Intramolecular n-type charge transfer has been observed by EPR in molecular thienyl-DPPs bound to an imidazolium bromide group [65] or tertiary amine [41]. The EPR signals of **DPPC8-X** (45 °C), **DPPC6-OH** (45 °C and 65 °C) and **DPPC8-OH** (45 °C and 65 °C) are similar but much broader. It is possible that changes in signal intensity between these samples could be due to morphological differences caused by film formation temperatures and differing sidechain lengths. It has been seen that charge transfer in trialkyl amine functionalised NDIs was highly dependent on the intramolecular distance between amine groups [68]. In both the hydroxide samples this could be further complicated by the changing chemical composition described above.

Samples of **DPPC6-X**, **DPPC8-X** (65 °C and 85 °C), **DPPC6-OH** (85 °C) and **DPP-C8-OH** (85 °C) exhibit slightly different EPR spectra with signals around 315 mT. For **DPPC6-OH** and **DPPC8-OH** the complicated chemical composition could lead to the presence of more than one type of free electron on different compounds in the mixture. Samples of **DPPC6-X** and **DPPC8-X** however are chemically pure. Again, morphological differences between chain lengths may be a factor but it also should be noted that anisotropy is exhibited in these films. Supplementary information Figure S31 shows EPR spectra of each sample rotated 90° and clear differences can be seen when compared to the original spectra. This anisotropy likely contributes to the broadening of the EPR signals and highlights that a complex morphology in many of these films plays a role in the doping mechanism (see Fig. 7 for examples of hydroxide films surface morphologies).

Further studies need to be conducted to fully elucidate the relationship between morphology and the nature of the charge transfer in these compounds. Unpaired electrons are also not stable over long lifetimes with measurements of **DPPC6-X** and **DPPC8-OH** retaken after 1 week storage in air showing a large decrease in signal intensity (Figure S32). This is not surprising since DPP small molecules are not expected to have electron affinities (EA) higher than the proposed 4.0 eV required to avoid reaction with ambient O_2 [69]. EPR spectra in Fig. 5. however support UV–vis absorption spectra showing that self-doping occurs in samples of **DPPC6-OH** and **DPPC8-OH**. While both **DPPC6-X** and **DPPC8-X** also clearly exhibit unpaired electrons in thin-films, giving a first indication of self-doping from the TFA ammonium hydroxide moiety as well.

Electrical conductivity, σ, values can provide insights into the extent of doping in semiconductors. The σ of thin films can be given as a product of the charge carrier mobility, μ, and the number of free charges generated, n. Linear four-point probe conductivity measurements were taken at room-temperature under ambient conditions and the results are summarised in Fig. 6. Films drop-cast at 125 °C were again omitted due to the assumption of degradation.

Samples of **DPPC6-OH** and **DPPC8-OH** gave conductivities of 2.81×10^{-4} and 3.25×10^{-4} S m^{-1} respectively for 45 °C drop-cast films (Fig. 6). Both then exhibited similar decreases in conductivity when processed at higher temperatures; down to approximately 1.00×10^{-5} S m^{-1} for both when films were drop-cast at 85 °C. The additional EPR signal around 315 mT in samples drop-cast at 85 °C did not translate to an increase in σ.

Films of **DPPC6-X** and **DPPC8-X** showed surprisingly high conductivities of 9.00×10^{-4} and 5.15×10^{-4} S m^{-1} respectively (both films cast at 45 °C). After annealing there was an initial decrease in conductivity at 65 °C. A significant increase was observed for films annealed at 85°C however, which gave conductivities of 1.29×10^{-3} S m^{-1} for **DPPC6-X** and 1.60×10^{-3} S m^{-1} for **DPPC8-X**. This was an order of magnitude increase when compared to the highest conductivities achieved in both hydroxide compounds

It is challenging to relate any trends seen in EPR measurements to trends seen in conductivities especially when considering the observed anisotropy (Figure S31). The complex interplay between chemical structure and morphology is likely contributing to the trends in conductivity seen in Fig. 6 and further study of the nature of the two EPR signals observed (315 mT and 332 mT) is required. The exact doping mechanism in these systems also warrants further investigation. From the observation of lower conductivities in hydroxide samples however it is likely that ammonium hydroxide decomposition reactions, such as Hoffmann elimination and demethylation [41,46], are not leading to products which are capable of efficiently doping DPPs. This may be due to a reduction in EA due to the ring-opening outlined in Scheme 3. The TFA precursors however are capable of intramolecular electron transfer, as exhibited by EPR and relatively high σ. This could simply be due to increased purity in these samples or to TFA anions being a previously unknown suitable dopant for DPPs.

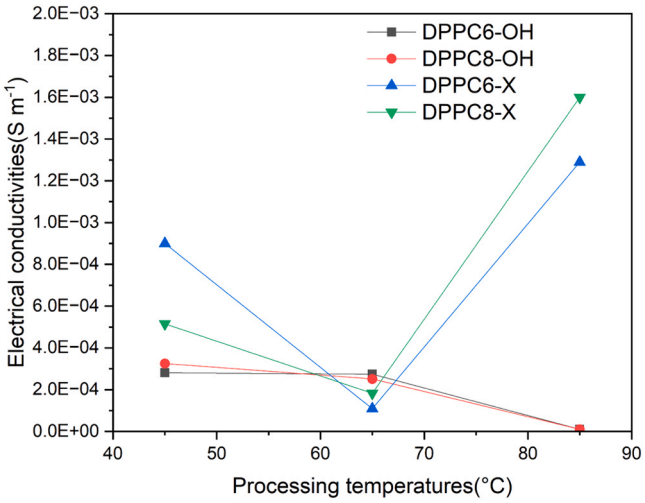

Fig. 6. Electrical conductivity of films of **DPPC6-X** and **DPPC8-X** drop-cast at 45°C and then annealed at 65 and 85°C and films of **DPPC6-OH** and **DPPC8-OH** drop-cast at 45, 65 and 85°C.

2.3. Film morphology

Conductivities of **DPPC6-OH** and **DPPC8-OH** were low but did not indicate that either were completely non-conducting. The presence of an EPR signal in all films further supports the presence of some unpaired electrons and hence some amount of self-doping. It was therefore decided that the morphology of the films should be investigated to elucidate the reason for relatively low conductivities in films containing unpaired electrons.

Atomic force microscopy (AFM) has been used here to image the surface morphology of **DPPC6-OH** and **DPPC8-OH** conducting films and are shown in Fig. 7. Both **DPPC6-OH** and **DPPC8-OH** at 45 °C and 65 °C show that surface morphology was dominated by fibrils which homogenously covered the substrate. This provides a good channel for charge transport and may go some way towards explaining higher conductivities at these drop-cast temperatures. Films at 85 °C however show the formation of separated particulates which break any effective channel for charge transport having a detrimental impact on μ and σ.

It is known that chemical impurities are a cause of charge carrier traps [70,71]. Even with more homogeneous morphologies seen in films at 45 °C and 65 °C the large number of chemical impurities present due to ring-opening are likely causing traps and leading to low conductivities seen in Fig. 6. The breakup of the surface morphology at 85 °C is likely due to the chemical decomposition at this temperature, both factors also contributing to the lower conductivities at these temperatures.

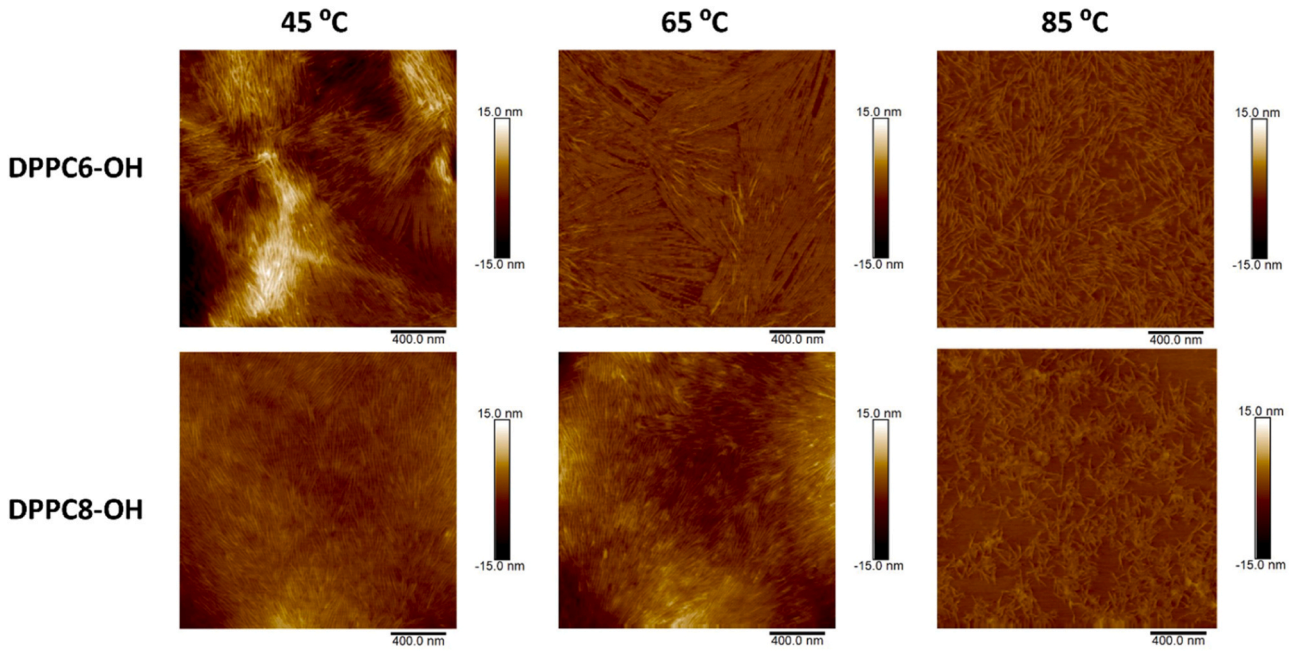

Fig. 7. Atomic force microscopy (AFM) height images of **DPPC6-OH** and **DPPC8-OH** thin films drop-cast at 45, 65 and 85°C.

3. Conclusions

Films of **DPPC6-OH** and **DPPC8-OH** have been shown to exhibit electronic conductivities under ambient conditions. N-type conductivities which are ambient stable are rare amongst organic semiconductors and provide a wealth of opportunities when considering multiple applications such as low temperature wearable thermoelectrics, OFETs or orthogonal solvent processable OPV layers. Incorporating these functionalities into polymer structures may provide further opportunities for the development of water soluble and ambient stable n-type materials.

Controlling the chemical composition of films functionalised with hydroxide anions is still a challenge due to the reversible hydrolysis reaction initiated by ion-exchange from the halide precursor. The lactam ring of DPP is theoretically inert to hydrolysis, however a significant amount of hydrolysis was still observed. It may be that it is only possible to circumvent this by removing the ion-exchange, using large excesses of hydroxide, from the synthesis completely. Sophisticated methods of electrodialysis are being developed for the efficient synthesis of quaternary ammonium hydroxides [72–74].

It should also be noted that the precursors **DPPC6-X** and **DPPC8-X** also gave conductivities while not exhibiting any of the chemical complexity of the hydroxides. The EPR signals under ambient conditions provide further evidence that quaternary ammonium groups provide exciting opportunities for n-type organic semiconductors. Since the TFA counterion gave higher conductivities than the hydroxide it could provide a more accessible choice of ion to be paired with other self-doping semiconductors such as rylene diimides. Since the complications of side reactions on amide and imide semiconducting cores are avoided, they may provide a promising alternative to hydroxides.

Funding

LMC, MMW, PAG-F, and BCS acknowledge funding from the UK Research and Innovation for Future Leaders Fellowship (MR/S031952/1). LMC and BCS would also like to acknowledge funding from the EPSRC (EP/W005875/1). IN and SH would like to acknowledge the EPSRC equipment funding for SPIN-Lab (EP/P030548/1). OF is funded by a Royal Society University Research Fellowship (UF140372 and URF/R/201013). PK-N is funded by a Dstl studentship.

CRediT authorship contribution statement

Lewis Matthew Cowen: Writing – original draft, Investigation, Data curation, Conceptualization. **Megan Mae Westwood:** Investigation, Data curation. **Pauline Kasongo-Ntumba:** Investigation, Data curation. **Irena Nevjestic:** Investigation, Data curation. **Peter Anthony Gilhooly-Finn:** Investigation, Data curation. **Sandrine Heutz:** Writing – review & editing, Supervision, Funding acquisition. **Oliver Fenwick:** Writing – review & editing, Supervision, Funding acquisition. **Bob Camille Schroeder:** Writing – review & editing, Supervision, Funding acquisition, Conceptualization.

Declaration of Competing Interest

The authors declare that they have no known competing financial interests or personal relationships that could have appeared to influence the work reported in this paper.

Data Availability

Data will be made available on request.

Appendix A. Supporting information

Supplementary data associated with this article can be found in the online version at doi:10.1016/j.synthmet.2024.117678.

References

[1] H. Shirakawa, E.J. Louis, A.G. MacDiarmid, C.K. Chiang, A.J. Heeger, Synthesis of electrically conducting organic polymers: halogen derivatives of polyacetylene, (CH), J. Chem. Soc. Chem. Commun. (16) (1977) 578–580.
[2] K. Walzer, B. Maennig, M. Pfeiffer, K. Leo, Highly efficient organic devices based on electrically doped transport layers, Chem. Rev. *107* (4) (2007) 1233–1271.
[3] J. Kido, T. Matsumoto, Bright organic electroluminescent devices having a metal-doped electron-injecting layer, Appl. Phys. Lett. *73* (20) (1998) 2866–2868.
[4] J. Huang, M. Pfeiffer, A. Werner, J. Blochwitz, K. Leo, S. Liu, Low-voltage organic electroluminescent devices using pin structures, Appl. Phys. Lett. *80* (1) (2002) 139–141.
[5] F. Ante, D. Kälblein, U. Zschieschang, T.W. Canzler, A. Werner, K. Takimiya, M. Ikeda, T. Sekitani, T. Someya, H. Klauk, Contact doping and ultrathin gate dielectrics for nanoscale organic thin-film transistors, Small *7* (9) (2011) 1186–1191.

[6] B. Maennig, M. Pfeiffer, A. Nollau, X. Zhou, K. Leo, P. Simon, Controlled p-type doping of polycrystalline and amorphous organic layers: self-consistent description of conductivity and field-effect mobility by a microscopic percolation model, Phys. Rev. B *64* (19) (2001) 195208.

[7] S. Olthof, S. Mehraeen, S.K. Mohapatra, S. Barlow, V. Coropceanu, J.-L. Brédas, S. R. Marder, A. Kahn, Ultralow doping in organic semiconductors: evidence of trap filling, Phys. Rev. Lett. *109* (17) (2012) 176601.

[8] A.F. Paterson, L. Tsetseris, R. Li, A. Basu, H. Faber, A.-H. Emwas, J. Panidi, Z. Fei, M.R. Niazi, D.H. Anjum, M. Heeney, T.D. Anthopoulos, Addition of the lewis acid zn(c6f5)2 enables organic transistors with a maximum hole mobility in excess of 20 cm2 V−1 s−1, Adv. Mater. *31* (27) (2019) 1900871.

[9] Y. Lin, Y. Firdaus, M.I. Nugraha, F. Liu, S. Karuthedath, A.-H. Emwas, W. Zhang, A. Seitkhan, M. Neophytou, H. Faber, E. Yengel, I. McCulloch, L. Tsetseris, F. Laquai, T.D. Anthopoulos, 17.1% efficient single-junction organic solar cells enabled by n-type doping of the bulk-heterojunction, Adv. Sci. *7* (7) (2020) 1903419.

[10] Y. Lin, Y. Zhang, J. Zhang, M. Marcinskas, T. Malinauskas, A. Magomedov, M. I. Nugraha, D. Kaltsas, D.R. Naphade, G.T. Harrison, A. El-Labban, S. Barlow, S. De Wolf, E. Wang, I. McCulloch, L. Tsetseris, V. Getautis, S.R. Marder, T. D. Anthopoulos, 18.9% efficient organic solar cells based on n-doped bulk-heterojunction and halogen-substituted self-assembled monolayers as hole extracting interlayers, Adv. Energy Mater. *12* (45) (2022) 2202503.

[11] J. Kong, Y. Shin, J.A. Röhr, H. Wang, J. Meng, Y. Wu, A. Katzenberg, G. Kim, D. Y. Kim, T.-D. Li, E. Chau, F. Antonio, T. Siboonruang, S. Kwon, K. Lee, J.R. Kim, M. A. Modestino, H. Wang, A.D. Taylor, CO2 doping of organic interlayers for perovskite solar cells, Nature *594* (7861)) (2021) 51–56.

[12] L.M. Cowen, J. Atoyo, M.J. Carnie, D. Baran, B.C. Schroeder, Review—organic materials for thermoelectric energy generation, ECS J. Solid State Sci. Technol. *6* (3) (2017) N3080–N3088.

[13] P.A. Finn, C. Asker, K. Wan, E. Bilotti, O. Fenwick, C.B. Nielsen, Thermoelectric materials: current status and future challenges, Front. Electron. Mater. *1* (2021).

[14] Y. Zhao, L. Liu, F. Zhang, C.-a Di, D. Zhu, Advances in organic thermoelectric materials and devices for smart applications, SmartMat *2* (4) (2021) 426–445.

[15] H. Bronstein, C.B. Nielsen, B.C. Schroeder, I. McCulloch, The role of chemical design in the performance of organic semiconductors, Nat. Rev. Chem. *4* (2) (2020) 66–77.

[16] J.E. Cochran, M.J.N. Junk, A.M. Glaudell, P.L. Miller, J.S. Cowart, M.F. Toney, C. J. Hawker, B.F. Chmelka, M.L. Chabinyc, Molecular interactions and ordering in electrically doped polymers: blends of PBTTT and F4TCNQ, Macromolecules *47* (19) (2014) 6836–6846.

[17] K. Kang, S. Watanabe, K. Broch, A. Sepe, A. Brown, I. Nasrallah, M. Nikolka, Z. Fei, M. Heeney, D. Matsumoto, K. Marumoto, H. Tanaka, Kuroda, S.-i.; Sirringhaus, H., 2D coherent charge transport in highly ordered conducting polymers doped by solid state diffusion, Nat. Mater. *15* (8) (2016) 896–902.

[18] S. Panigrahy, B. Kandasubramanian, Polymeric thermoelectric PEDOT: PSS & composites: synthesis, progress, and applications, Eur. Polym. J. *132* (2020) 109726.

[19] Z. Fan, J. Ouyang, Thermoelectric properties of PEDOT:PSS, Adv. Electron. Mater. *5* (11) (2019) 1800769.

[20] S.N. Patel, A.M. Glaudell, K.A. Peterson, E.M. Thomas, K.A. O'Hara, E. Lim, M. L. Chabinyc, Morphology controls the thermoelectric power factor of a doped semiconducting polymer, Sci. Adv. *3* (6) (2017) e1700434.

[21] E. Lim, K.A. Peterson, G.M. Su, M.L. Chabinyc, Thermoelectric properties of poly(3-hexylthiophene) (P3HT) doped with 2,3,5,6-tetrafluoro-7,7,8,8-tetracyanoquino-dimethane (F4TCNQ) by vapor-phase infiltration, Chem. Mater. *30* (3) (2018) 998–1010.

[22] D.S. Maddison, R.B. Roberts, J. Unsworth, Thermoelectric power of polypyrrole, Synth. Met. *33* (3) (1989) 281–287.

[23] K. Bender, E. Gogu, I. Hennig, D. Schweitzer, H. Müenstedt, Electric conductivity and thermoelectric power of various polypyrroles, Synth. Met. *18* (1) (1987) 85–88.

[24] S.A. Gregory, A.K. Menon, S. Ye, D.S. Seferos, J.R. Reynolds, S.K. Yee, Effect of heteroatom and doping on the thermoelectric properties of poly(3-alkylchalcogenophenes), Adv. Energy Mater. *8* (34) (2018) 1802419.

[25] Q. Yao, Q. Wang, L. Wang, Y. Wang, J. Sun, H. Zeng, Z. Jin, X. Huang, L. Chen, The synergic regulation of conductivity and Seebeck coefficient in pure polyaniline by chemically changing the ordered degree of molecular chains, J. Mater. Chem. A *2* (8) (2014) 2634–2640.

[26] I.H. Jung, C.T. Hong, U.-H. Lee, Y.H. Kang, K.-S. Jang, S.Y. Cho, High thermoelectric power factor of a diketopyrrolopyrrole-based low bandgap polymer via finely tuned doping engineering, Sci. Rep. *7* (1) (2017) 44704.

[27] Y. Wang, M. Nakano, T. Michinobu, Y. Kiyota, T. Mori, K. Takimiya, Naphthodithiophenediimide–benzobisthiadiazole-based polymers: versatile n-type materials for field-effect transistors and thermoelectric devices, Macromolecules *50* (3) (2017) 857–864.

[28] J. Liu, L. Qiu, R. Alessandri, X. Qiu, G. Portale, J. Dong, W. Talsma, G. Ye, A. A. Sengrian, P.C.T. Souza, M.A. Loi, R.C. Chiechi, S.J. Marrink, J.C. Hummelen, L.J. A. Koster, Enhancing molecular n-type doping of donor–acceptor copolymers by tailoring side chains, Adv. Mater. *30* (7) (2018) 1704630.

[29] R.A. Schlitz, F.G. Brunetti, A.M. Glaudell, P.L. Miller, M.A. Brady, C.J. Takacs, C. J. Hawker, M.L. Chabinyc, Solubility-limited extrinsic n-type doping of a high electron mobility polymer for thermoelectric applications, Adv. Mater. *26* (18) (2014) 2825–2830.

[30] Y. Song, J. Ding, X. Dai, C. Li, C.-a Di, D. Zhang, , Enhancement of the thermoelectric performance of n-type naphthalene diimide-based conjugated polymer by engineering of side alkyl chains. *ACS*, Mater. Lett. *4* (4) (2022) 521–527.

[31] K. Shi, F. Zhang, C.-A. Di, T.-W. Yan, Y. Zou, X. Zhou, D. Zhu, J.-Y. Wang, J. Pei, Toward high performance n-type thermoelectric materials by rational modification of BDPPV backbones, J. Am. Chem. Soc. *137* (22) (2015) 6979–6982.

[32] X. Zhao, D. Madan, Y. Cheng, J. Zhou, H. Li, S.M. Thon, A.E. Bragg, M.E. DeCoster, P.E. Hopkins, H.E. Katz, High conductivity and electron-transfer validation in an n-type fluoride-anion-doped polymer for thermoelectrics in air, Adv. Mater. *29* (34) (2017) 1606928.

[33] B.D. Naab, S. Guo, S. Olthof, E.G.B. Evans, P. Wei, G.L. Millhauser, A. Kahn, S. Barlow, S.R. Marder, Z. Bao, Mechanistic study on the solution-phase n-doping of 1,3-dimethyl-2-aryl-2,3-dihydro-1h-benzoimidazole derivatives, J. Am. Chem. Soc. *135* (40) (2013) 15018–15025.

[34] B.D. Naab, S. Zhang, K. Vandewal, A. Salleo, S. Barlow, S.R. Marder, Z. Bao, Effective solution- and vacuum-processed n-doping by dimers of benzimidazoline radicals, Adv. Mater. *26* (25) (2014) 4268–4272.

[35] S. Zhang, B.D. Naab, E.V. Jucov, S. Parkin, E.G.B. Evans, G.L. Millhauser, T. V. Timofeeva, C. Risko, J.-L. Brédas, Z. Bao, S. Barlow, S.R. Marder, n-dopants based on dimers of benzimidazoline radicals: structures and mechanism of redox reactions, Chem. – A Eur. J. *21* (30) (2015) 10878–10885.

[36] J. Liu, Y. Shi, J. Dong, M.I. Nugraha, X. Qiu, M. Su, R.C. Chiechi, D. Baran, G. Portale, X. Guo, L.J.A. Koster, Overcoming coulomb interaction improves free-charge generation and thermoelectric properties for n-doped conjugated polymers, ACS Energy Lett. *4* (7) (2019) 1556–1564.

[37] B.A. Gregg, R.A. Cormier, Doping molecular semiconductors: n-type doping of a liquid crystal perylene diimide, J. Am. Chem. Soc. *123* (32) (2001) 7959–7960.

[38] B.A. Gregg, S.-G. Chen, R.A. Cormier, Coulomb forces and doping in organic semiconductors, Chem. Mater. *16* (23) (2004) 4586–4599.

[39] T.H. Reilly, A.W. Hains, H.-Y. Chen, B.A. Gregg, A self-doping, O2-stable, n-type interfacial layer for organic electronics, Adv. Energy Mater. *2* (4) (2012) 455–460.

[40] B. Russ, M.J. Robb, F.G. Brunetti, P.L. Miller, E.E. Perry, S.N. Patel, V. Ho, W. B. Chang, J.J. Urban, M.L. Chabinyc, C.J. Hawker, R.A. Segalman, Power factor enhancement in solution-processed organic n-type thermoelectrics through molecular design, Adv. Mater. *26* (21) (2014) 3473–3477.

[41] B. Russ, M.J. Robb, B.C. Popere, E.E. Perry, C.-K. Mai, S.L. Fronk, S.N. Patel, T. E. Mates, G.C. Bazan, J.J. Urban, M.L. Chabinyc, C.J. Hawker, R.A. Segalman, Tethered tertiary amines as solid-state n-type dopants for solution-processable organic semiconductors, Chem. Sci. *7* (3) (2016) 1914–1919.

[42] D. Powell, X. Zhang, C.I. Nwachukwu, E.J. Miller, K.R. Hansen, L. Flannery, J. Ogle, A. Berzansky, J.G. Labram, A.G. Roberts, L. Whittaker-Brooks, Establishing self-dopant design principles from structure–function relationships in self-n-doped perylene diimide organic semiconductors, Adv. Mater. *34* (42) (2022) 2204656.

[43] J.B. Edson, C.S. Macomber, B.S. Pivovar, J.M. Boncella, Hydroxide based decomposition pathways of alkyltrimethylammonium cations, J. Membr. Sci. *399-400* (2012) 49–59.

[44] S. Chempath, B.R. Einsla, L.R. Pratt, C.S. Macomber, J.M. Boncella, J.A. Rau, B. S. Pivovar, Mechanism of tetraalkylammonium headgroup degradation in alkaline fuel cell membranes, J. Phys. Chem. C. *112* (9) (2008) 3179–3182.

[45] S. Chempath, J.M. Boncella, L.R. Pratt, N. Henson, B.S. Pivovar, Density functional theory study of degradation of tetraalkylammonium hydroxides, J. Phys. Chem. C. *114* (27) (2010) 11977–11983.

[46] L.M. Cowen, P.A. Gilhooly-Finn, A. Giovannitti, G. LeCroy, H. Demetriou, W. Neal, Y. Dong, M. Westwood, S. Luong, O. Fenwick, A. Salleo, S. Heutz, C.B. Nielsen, B. C. Schroeder, Critical analysis of self-doping and water-soluble n-type organic semiconductors: structures and mechanisms, J. Mater. Chem. C. *10* (23) (2022) 8955–8963.

[47] L. Chen, Y. Tan, X. Liu, Y. Chen, Counterion induced facile self-doping and tunable interfacial dipoles of small molecular electrolytes for efficient polymer solar cells, Nano Energy *27* (2016) 492–498.

[48] C.-Y. Yang, W.-L. Jin, J. Wang, Y.-F. Ding, S. Nong, K. Shi, Y. Lu, Y.-Z. Dai, F.-D. Zhuang, T. Lei, C.-A. Di, D. Zhu, J.-Y. Wang, J. Pei, Enhancing the n-type conductivity and thermoelectric performance of donor–acceptor copolymers through donor engineering, Adv. Mater. *30* (43) (2018) 1802850.

[49] X. Yan, M. Xiong, J.-T. Li, S. Zhang, Z. Ahmad, Y. Lu, Z.-Y. Wang, Z.-F. Yao, J.-Y. Wang, X. Gu, T. Lei, Pyrazine-flanked diketopyrrolopyrrole (DPP): a new polymer building block for high-performance n-type organic thermoelectrics, J. Am. Chem. Soc. *141* (51) (2019) 20215–20221.

[50] K. Pu, J. Mei, J.V. Jokerst, G. Hong, A.L. Antaris, N. Chattopadhyay, A. J. Shuhendler, T. Kurosawa, Y. Zhou, S.S. Gambhir, Z. Bao, J. Rao, Diketopyrrolopyrrole-based semiconducting polymer nanoparticles for in vivo photoacoustic imaging, Adv. Mater. *27* (35) (2015) 5184–5190.

[51] Q. Liu, S.E. Bottle, P. Sonar, Developments of diketopyrrolopyrrole-dye-based organic semiconductors for a wide range of applications in electronics, Adv. Mater. *32* (4) (2020) 1903882.

[52] W.W. Bao, R. Li, Z.C. Dai, J. Tang, X. Shi, J.T. Geng, Z.F. Deng, J. Hua, Diketopyrrolopyrrole (DPP)-based materials and its applications: a review, Front. Chem. *8* (2020).

[53] J. Xu, B. Chen, J. Lv, D. Chang, D. Niu, S. Hu, X. Zhang, Z. Xin, L. Wang, Aryl modification of diketopyrrolopyrrole-based quaternary ammonium salts and their applications in copper electrodeposition, Dyes Pigments *170* (2019) 107559.

[54] Williams, M., The Merck Index: An Encyclopedia of Chemicals, Drugs, and Biologicals, 15th Edition Edited by M.J. O'Neil, Royal Society of Chemistry, Cambridge, UK ISBN 9781849736701; 2708 pages. April 2013, $150 with 1-year free access to The Merck Index Online. *Drug Development Research* 2013, *74* (5), 339-339.

[55] V.V. Andrushchenko, H.J. Vogel, E.J. Prenner, Optimization of the hydrochloric acid concentration used for trifluoroacetate removal from synthetic peptides, J. Pept. Sci. *13* (1) (2007) 37–43.
[56] G. Li, S. Ma, M. Szostak, Amide bond activation: the power of resonance, Trends Chem. *2* (10) (2020) 914–928.
[57] L. Pauling, The nature of the chemical bond. II. The one-electron bond and the three-electron bond, J. Am. Chem. Soc. *53* (9) (1931) 3225–3237.
[58] H.A. Staab, New methods of preparative organic chmistry IV. Syntheses using heterocyclic amides (Azolides), Angew. Chem. Int. Ed. Engl. *1* (7) (1962) 351–367.
[59] J.P. Lee, R. Bembi, T.H. Fife, Steric effects in the hydrolysis reactions of N-acylimidazoles. Effect of aryl substitution in the leaving group, J. Org. Chem. *62* (9) (1997) 2872–2876.
[60] E.A. Stone, B.Q. Mercado, S.J. Miller, Structure and reactivity of highly twisted N-acylimidazoles, Org. Lett. *21* (7) (2019) 2346–2351.
[61] F.M. Menger, J.A. Donohue, Base-catalyzed hydrolysis of N-acylpyrroles. Measurable acidity of a steady-state tetrahedral intermediate, J. Am. Chem. Soc. *95* (2) (1973) 432–437.
[62] A.M. Goldys, C.S.P. McErlean, N-acylpyrroles: more than amides, Eur. J. Org. Chem. *2012* (10) (2012) 1877–1888.
[63] Z. Zeng, X. Shi, C. Chi, J.T. López Navarrete, J. Casado, J. Wu, Pro-aromatic and anti-aromatic π-conjugated molecules: an irresistible wish to be diradicals, Chem. Soc. Rev. *44* (18) (2015) 6578–6596.
[64] K.J. Fallon, P. Budden, E. Salvadori, A.M. Ganose, C.N. Savory, L. Eyre, S. Dowland, Q. Ai, S. Goodlett, C. Risko, D.O. Scanlon, C.W.M. Kay, A. Rao, R. H. Friend, A.J. Musser, H. Bronstein, Exploiting excited-state aromaticity to design highly stable singlet fission materials, J. Am. Chem. Soc. *141* (35) (2019) 13867–13876.
[65] D. Zhou, Y. Li, H. Zhang, H. Zheng, X. Shen, W. You, L. Hu, L. Han, Y. Tong, L. Chen, N-type small molecule electron transport materials with D-A-D conjugated core for non-fullerene organic solar cells, Chem. Eng. J. *452* (2023) 139260.
[66] M. Stolte, S.-L. Suraru, P. Diemer, T. He, C. Burschka, U. Zschieschang, H. Klauk, F. Würthner, Diketopyrrolopyrrole organic thin-film transistors: impact of alkyl substituents and tolerance of ethylhexyl stereoisomers, Adv. Funct. Mater. *26* (41) (2016) 7415–7422.
[67] J.L. Bredas, G.B. Street, Polarons, bipolarons, and solitons in conducting polymers, Acc. Chem. Res. *18* (10) (1985) 309–315.
[68] Y. Matsunaga, K. Goto, K. Kubono, K. Sako, T. Shinmyozu, Photoinduced color change and photomechanical effect of naphthalene diimides bearing alkylamine moieties in the solid state, Chem. – A Eur. J. *20* (24) (2014) 7309–7316.
[69] H. Usta, C. Risko, Z. Wang, H. Huang, M.K. Deliomeroglu, A. Zhukhovitskiy, A. Facchetti, T.J. Marks, Design, synthesis, and characterization of ladder-type molecules and polymers. air-stable, solution-processable n-channel and ambipolar semiconductors for thin-film transistors via experiment and theory, J. Am. Chem. Soc. *131* (15) (2009) 5586–5608.
[70] H.F. Haneef, A.M. Zeidell, O.D. Jurchescu, Charge carrier traps in organic semiconductors: a review on the underlying physics and impact on electronic devices, J. Mater. Chem. C. *8* (3) (2020) 759–787.
[71] O. Sachnik, X. Tan, D. Dou, C. Haese, N. Kinaret, K.-H. Lin, D. Andrienko, M. Baumgarten, R. Graf, G.-J.A.H. Wetzelaer, J.J. Michels, P.W.M. Blom, Elimination of charge-carrier trapping by molecular design, Nat. Mater. (2023).
[72] H. Feng, C. Huang, T. Xu, Production of tetramethyl ammonium hydroxide using bipolar membrane electrodialysis, Ind. Eng. Chem. Res. *47* (20) (2008) 7552–7557.
[73] J. Shen, J. Yu, L. Liu, J. Lin, B. Van der Bruggen, Synthesis of quaternary ammonium hydroxide from its halide salt by bipolar membrane electrodialysis (BMED): effect of molecular structure of ammonium compounds on the process performance, J. Chem. Technol. Biotechnol. *89* (6) (2014) 841–850.
[74] J. Shen, Z. Hou, C. Gao, Using bipolar membrane electrodialysis to synthesize di-quaternary ammonium hydroxide and optimization design by response surface methodology, Chin. J. Chem. Eng. *25* (9) (2017) 1176–1181.